Supporting Information

For the manuscript entitled:

A general screening strategy for peptide-based fluorogenic ligands: Probes for the dynamic studies of PDZ domain-mediated interactions

Matthieu Sainlos,[†] Wendy S. Iskenderian,[†] and Barbara Imperiali[†,‡]*

[†]*Department of Chemistry and* [‡]*Department of Biology, Massachusetts Institute of Technology, 77 Massachusetts Avenue, Cambridge, Massachusetts 02139-4307, USA*

*Author to whom correspondence should be addressed; e-mail: imper@mit.edu

Contents

Supporting Figure S1

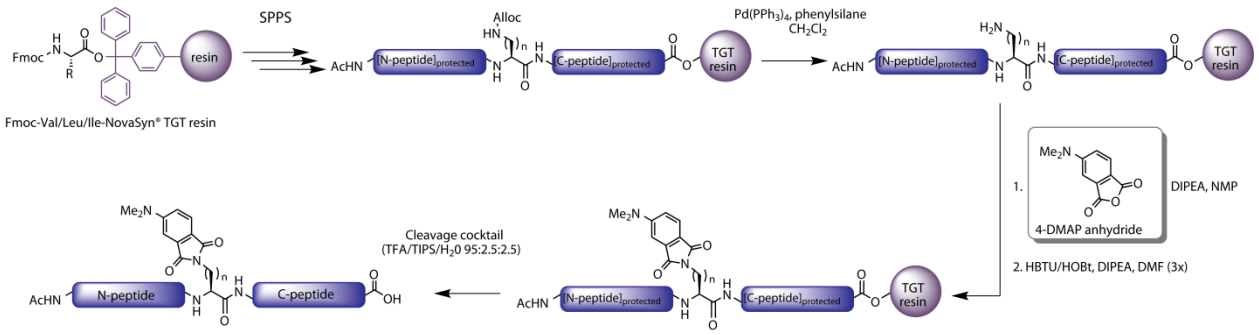

Supporting Figure S1. General method for environment-sensitive PDZ domain probe synthesis (n= 1, Dap; n=2, Dab; n=3, Orn).

Supporting Table S2

Entry #	Original sequence	Sequence[a] -12 -11 -10 -9 -8 -7 -6 -5 -4 -3 -2 -1 0	Fomula	Mass[b] expected M	Mass[b] obtained [MH]$^+$	t_R[c]
1	Stargazin	Ac- N T A N R R T T α V -COOH	$C_{55}H_{88}N_{20}O_{19}$	1332.7	1333.5	21.8
2	Stargazin	Ac- N T A N R R α T P V -COOH	$C_{56}H_{88}N_{20}O_{18}$	1328.7	1330.5	21.7
3	Stargazin	Ac- N T A N R α T T P V -COOH	$C_{54}H_{83}N_{17}O_{19}$	1273.6	1274.6	22.1
4	Stargazin	Ac- N T A N R β T T P V -COOH	$C_{55}H_{85}N_{17}O_{19}$	1287.6	1288.8	22.4
5	Stargazin	Ac- N T A N α R T T P V -COOH	$C_{54}H_{83}N_{17}O_{19}$	1273.6	1275.6	21.8
6	Stargazin	Ac- N T A N β R T T P V -COOH	$C_{55}H_{85}N_{17}O_{19}$	1287.6	1288.6	22.6
7	Stargazin	Ac- N T A N γ R T T P V -COOH	$C_{56}H_{87}N_{17}O_{19}$	1301.6	1302.7	22.6
8	Stargazin	Ac- N T A β R R T T P V -COOH	$C_{57}H_{91}N_{19}O_{18}$	1329.7	1330.7	23.0
9	Stargazin	Ac- N T β N R R T T P V -COOH	$C_{58}H_{92}N_{20}O_{19}$	1372.7	1373.6	21.7
10	Stargazin	Ac- N β A N R R T T P V -COOH	$C_{57}H_{90}N_{20}O_{18}$	1342.7	1343.5	21.8
11	Stargazin	Ac- β T A N R R T T P V -COOH	$C_{57}H_{91}N_{19}O_{18}$	1329.7	1331.0	22.7
12	Stargazin	Ac- *N R R* N T A N β R T T P V -COOH	$C_{71}H_{115}N_{27}O_{23}$	1713.9	1714.4	22.7
13	NR2a	Ac- *N R R* K K λ P β I E S D V -COOH	$C_{78}H_{128}N_{24}O_{23}$	1769.0	1769.9	23.7
14	CRIPT	Ac- D T K N β K Q T S V -COOH	$C_{57}H_{90}N_{16}O_{21}$	1334.7	1335.7	20.5
15	GluR1	Ac- *N R R* S G λ P β G A T G L -COOH	$C_{65}H_{104}N_{22}O_{20}$	1512.8	1513.7	24.1
16	Stargazin	Ac- *N R R* N T A N β R T R P R -NH2	$C_{74}H_{123}N_{33}O_{22}$	1826.0	1826.5	19.5
17	mGluR7a	Ac- A K K K Y V S β N N L V I -COOH	$C_{79}H_{126}N_{20}O_{21}$	1690.9	1692.6	24.0
18	Stargazin	Ac- φ N T A N R R T T P V -COOH	$C_{56}H_{90}N_{20}O_{20}$	1362.7	1363.4	21.1
19	GluR1	Ac- φ *N R R* S G λ P L G A T G L -COOH	$C_{66}H_{108}N_{22}O_{21}$	1545.7	1545.2	26.1
20	CRIPT	Ac- φ D T K N Y K Q T S V -COOH	$C_{61}H_{92}N_{16}O_{23}$	1416.7	1417.7	22.2

Supporting Table S2. Peptide listing and characterization. [a]Critical residues (position 0 and -2) are in red, native methionine residues were replaced by norleucine, α = Dap(4-DMAP), β = Dab(4-DMAP), γ = Orn(4-DMAP), λ = norleucine, φ = *p*-nitrophenylalanine, the *NRR* sequence was added on the N-terminus to improve solubility at high concentrations since low solubility of the probe can lead to high background fluorescence signal due to aggregation. [b] Masses were determinated by MALDI-TOF spectroscopy. [c] Retention times from analytical reverse phase HPLC (YMC C_{18}, ODS-A 5/120, 250 × 4.6 mm) using a standard gradient (5% acetonitrile containing 0.1% TFA for 5 min followed by a gradient from 5 to 95% acetonitrile containing 0.1% TFA over 35 min in water containing 0.1% TFA at a flow rate of 1 mL.min^{-1}). All the peptides were more than 95% pure as judged by analytical HPLC.

Supporting Figure S3

A

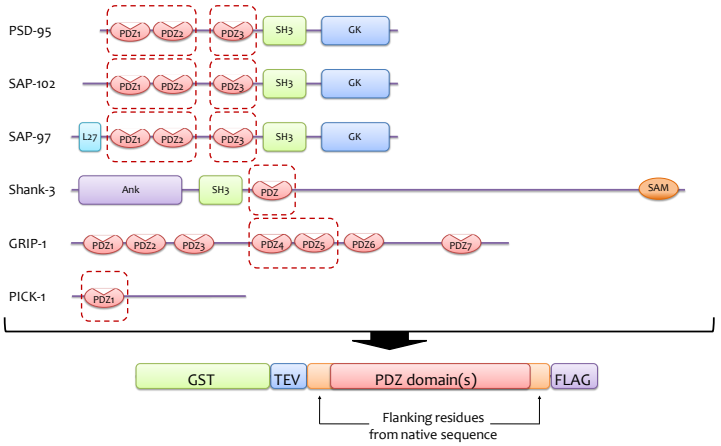

B

Single domain sequences alignment:

```
                1                                                  50
PSD95-3         LGEEDIPREP RRIVIHRGST GLGFNIVGG. .......... .EDGEGIFIS
SAP97-3         LGDDEITREP RKVVLHRGST GLGFNIVGG. .......... .EDGEGIFIS
SAP102-3        LAEEDFTREP RKIILHKGST GLGFNIVGG. .......... .EDGEGIFVS
Shank3          SHSDYVIDDK VAILQKRDHE GFGFVLRGAK AETPIEEFTP TPAFPALQYL
PICK1           EDKLGIPTVP GKVTLQKDAQ NLIGISIGGG .......... AQYCPCLYIV

                51                                                 100
PSD95-3         FILAGGPADL SGELRKGDQI LSVNGVDLRN ASHEQAAIAL KNAGQTVTII
SAP97-3         FILAGGPADL SGELRKGDRI ISVNSVDLRA ASHEQAAAAL KNAGQAVTIV
SAP102-3        FILAGGPADL SGELRRGDRI LSVNGVNLRN ATHEQAAAAL KRAGQSVTIV
Shank3          ESVDVEGVAW KAGLRTGDFL IEVNGVNVVK VGHKQVVGLI RQGGNRLVMK
PICK1           QVFDNTPAAL DGTVAAGDEI TGVNGRSIKG KTKVEVAKMI QEVKGEVTIH

                101             115
PSD95-3         AQYKPEEYSR FEA..
SAP97-3         AQYRPEEYSR FEA..
SAP102-3        AQYRPEEYSR FES..
Shank3          VVSVTRKPEE DSARR
PICK1           YNKLQADPKQ GMS..
```

Tandem domain sequences alignment:

```
                1                                                  50
PSD95-12        .......... .......... .......... ........ME YEEITLERGN
SAP97-12        .......... .......... .......... .....DADYE YEEITLERGN
SAP102-12       .......... .......... .......... ..NGSDGMFK YEEIVLERGN
GRIP-45         STSPRGTMMR RRLKKKDFKS SLSLASSTVG LAGQVVHTET TEVVLTADPV

                51                                                 100
PSD95-12        SGLGFSIAGG TDNPHIGDDP SIFITKIIPG GAAAQDGRLR VNDSILFVNE
SAP97-12        SGLGFSIAGG TDNPHIGDDS SIFITKIITG GAAAQDGRLR VNDCILRVNE
SAP102-12       SGLGFSIAGG IDNPHVPDDP GIFITKIIPG GAAAMDGRLG VNDCVLRVNE
GRIP-45         TGFGIQLQGS VFATETLSSP PL.ISYIEAD SPAERCGVLQ IGDRVMAING

                101                                                150
PSD95-12        VDVREVTHSA AVEALKEAGS IVRLYVMRRK PPAEKVMEIK .....LIKGP
SAP97-12        ADVRDVTHSK AVEALKEAGS IVRLYVKRRK PASEKIMEIK .....LIKGP
SAP102-12       VDVSEVVHSR AVEALKEAGP VVRLVVRRRQ PPPETIMEVN .....LLKGP
GRIP-45         IPTEDSTFEE ANQLLRDSSI TSKVTLEIEF DVAESVIPSS GTFHVKLPKK

                151                                                200
PSD95-12        KGLGFSIAGG VGNQHIPGDN SIYVTKIIEG GAAHKDGRLQ IGDKILAVNS
SAP97-12        KGLGFSIAGG VGNQHIPGDN SIYVTKIIEG GAAHKDGKLQ IGDKLLAVNS
SAP102-12       KGLGFSIAGG IGNQHIPGDN SIYITKIIEG GAAQKDGRLQ IGDRLLAVNN
GRIP-45         HSVELGITIS SPSSRKPGD. PLVISDIKKG SVAHRTGTLE LGDKLLAIDN

                201                                    237
PSD95-12        VGLEDVMHED AVAALKNTYD VVYLKVAKPS NA.....
SAP97-12        VCLEEVTHEE AVTALKNTSD FVYLKVAKPT SMYINDG
SAP102-12       TNLQDVRHEE AVASLKNTSD MVYLKVAKPG SLHLNDM
GRIP-45         IRLDSCSMED AVQILQQCED LVKLKIRKDE DNSDEQE
```

C

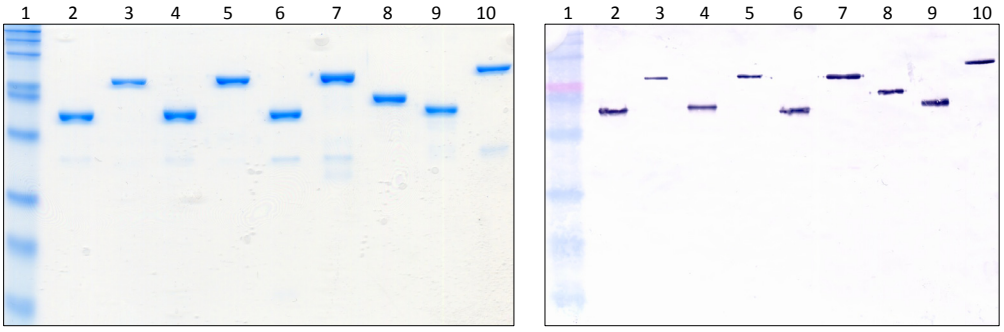

Supporting Figure S3. Recombinant PDZ domains. (**A**) PDZ domain-containing proteins used in this study and common construct used for the expressed domains. (**B**) Alignment of the expressed single and tandem PDZ domains sequences. (**C**) 12% SDS-PAGE of expressed PDZ domains (Coomassie staining and anti-FLAG Western Blot). Lane **1**: ladder; **2**: PSD95-3 (38955 kDa); **3**: PSD95-12 (48236 kDa); **4**: SAP97-3 (38860 kDa); **5**: SAP97-12 (49232 kDa); **6**: SAP102-3 (39036 kDa); **7**: SAP102-12 (49429 kDa); **8**: Shank3 (40821 kDa); **9**: PICK1 (38977 kDa); **10**: GRIP-45 (53546 kDa).

Supporting Figure S4

A

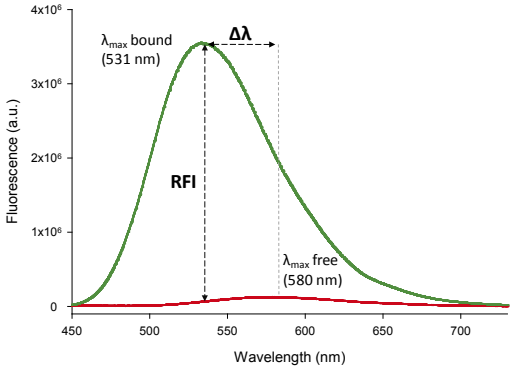

B

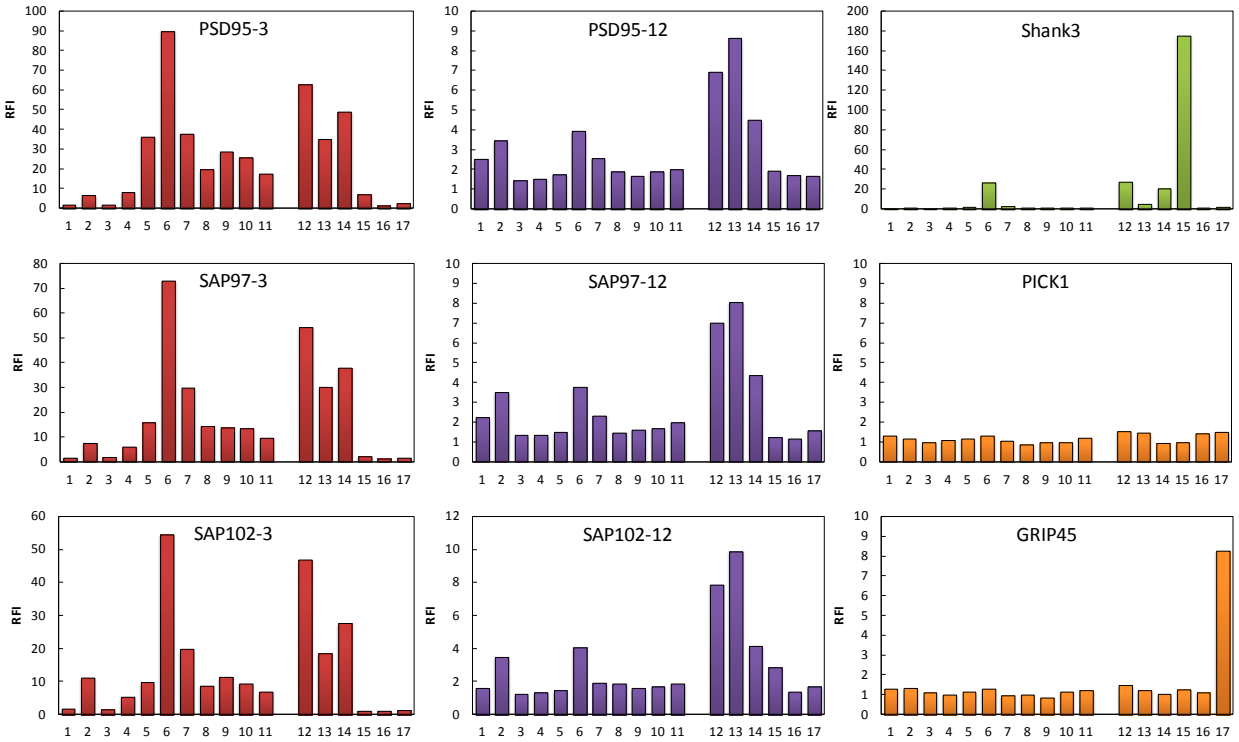

Supporting Figure S4. Relative fluorescence increases (RFI). (**A**) Example of fluorescence increase obtained with peptide **12**. Red line: peptide **12** in PBS (2 μM); green line: peptide **12** in PBS (2 μM) + PSD95-3 (20 μM). The relative fluorescence increase is defined by the ratio of $I^{bound}(\lambda_{max\ bound})/ I^{free}(\lambda_{max\ bound})$ where the fluorescence intensities I^{bound} and I^{free} are obtained by averaging at least three independent measurements and are calculated over a range of 5 nm centered around $\lambda_{max\ bound}$. (**B**) Relative fluorescence increases (RFI) obtained with all expressed PDZ domains.

Supporting Figure S5

A

#	PSD95-3		PSD95-12		SAP97-3		SAP97-12		SAP102-3		SAP102-12		Shank3		PICK		GRIP45	
	RFI[a]	Δλ [b]	RFI[a]	Δλ [b]	RFI[a]	Δλ [b]	RFI[a]	Δλ [b]	RFI[a]	Δλ [b]	RFI[a]	Δλ [b]	RFI[a]	Δλ [b]	RFI[a]	Δλ [b]	RFI[a]	Δλ [b]
1	1.9	*14*	2.5	*17*	1.6	*12*	2.3	*14*	1.8	*12*	1.6	*9*	1.0	*2*	1.3	*4*	1.3	*4*
2	6.6	*31*	3.4	*21*	7.5	*33*	3.5	*23*	11.2	*37*	3.5	*25*	1.1	*1*	1.2	*3*	1.3	*4*
3	1.7	*10*	1.5	*6*	1.8	*12*	1.3	*6*	1.5	*8*	1.2	*2*	1.0	*0*	1.0	*0*	1.1	*1*
4	8.0	*36*	1.5	*10*	6.2	*34*	1.4	*11*	5.3	*31*	1.4	*10*	1.5	*1*	1.1	*0*	1.0	*1*
5	36.1	*57*	1.8	*10*	15.8	*48*	1.5	*9*	9.9	*43*	1.5	*10*	2.0	*9*	1.2	*3*	1.1	*2*
6	**89.5**	*50*	3.9	*26*	**73.1**	*50*	3.8	*28*	**54.5**	*49*	4.1	*28*	26.7	*36*	1.3	*4*	1.3	*0*
7	37.6	*48*	2.6	*22*	29.8	*47*	2.3	*20*	19.9	*45*	1.9	*20*	3.0	*17*	1.1	*3*	1.0	*1*
8	19.8	*40*	1.9	*17*	14.3	*36*	1.5	*10*	8.6	*35*	1.9	*17*	1.2	*4*	0.9	*2*	1.0	*1*
9	28.7	*47*	1.7	*13*	13.7	*41*	1.6	*13*	11.3	*43*	1.6	*13*	1.3	*3*	1.0	*4*	0.9	*2*
10	25.6	*45*	1.9	*13*	13.6	*41*	1.7	*11*	9.5	*38*	1.7	*12*	1.3	*2*	1.0	*2*	1.1	*2*
11	17.4	*45*	2.0	*16*	9.5	*41*	2.0	*14*	7.0	*35*	1.9	*15*	1.3	*6*	1.2	*1*	1.2	*3*
12	62.6	*48*	6.9	*33*	54.3	*48*	7.0	*34*	46.8	*47*	7.9	*36*	27.6	*41*	1.5	*6*	1.5	*4*
13	35.1	*41*	**8.6**	*37*	30.2	*41*	**8.0**	*36*	18.5	*41*	**9.8**	*37*	4.9	*32*	1.4	*11*	1.2	*5*
14	48.8	*46*	4.5	*31*	38.0	*46*	4.4	*30*	27.6	*46*	4.2	*30*	21.0	*41*	0.9	*2*	1.0	*1*
15	4.6	*38*	1.9	*17*	2.2	*23*	1.3	*8*	1.2	*7*	2.8	*39*	**265.0**	*69*	1.0	*5*	1.3	*11*
16	1.4	*7*	1.7	*9*	1.4	*6*	1.2	*4*	1.0	*3*	1.4	*6*	1.5	*1*	1.4	*13*	1.1	*2*
17	2.7	*24*	1.7	*10*	1.7	*12*	1.6	*8*	1.4	*7*	1.7	*8*	1.9	*5*	1.5	*9*	**8.2**	*32*

B

#	*apo*		PSD95-3		PSD95-12		SAP97-3		SAP97-12		SAP102-3		SAP102-12		Shank3		PICK		GRIP45	
	λ	FI[c]	λ	FI[c]	λ	FI[c]	λ	FI[c]	λ	FI[c]	λ	FI[c]	λ	FI[c]	λ	FI[c]	λ	FI[c]	λ	FI[c]
1	*562*	9.12×10^{4} ±3.6×10^{3}	*548*	1.64×10^{5} ±3.6×10^{3}	*545*	2.15×10^{5} ±8.8×10^{3}	*550*	1.40×10^{5} ±2.8×10^{3}	*548*	1.95×10^{5} ±1.1×10^{4}	*550*	1.56×10^{5} ±8.5×10^{3}	*553*	1.42×10^{5} ±3.9×10^{3}	*560*	6.88×10^{4} ±1.2×10^{3}	*558*	1.19×10^{5} ±2.6×10^{3}	*558*	1.17×10^{5} ±2.2×10^{3}
2	*573*	5.43×10^{4} ±1.8×10^{3}	*542*	2.71×10^{5} ±1.4×10^{4}	*552*	1.67×10^{5} ±7.1×10^{3}	*540*	3.00×10^{5} ±1.4×10^{4}	*550*	1.65×10^{5} ±7.8×10^{3}	*536*	4.20×10^{5} ±1.1×10^{4}	*548*	1.58×10^{5} ±3.5×10^{3}	*572*	4.63×10^{4} ±7.9×10^{2}	*570*	6.34×10^{4} ±2.2×10^{3}	*569*	7.20×10^{4} ±1.4×10^{3}
3	*572*	6.64×10^{4} ±2.6×10^{3}	*562*	1.07×10^{5} ±4.8×10^{3}	*566*	9.52×10^{4} ±2.3×10^{3}	*560*	1.14×10^{5} ±4.2×10^{3}	*566*	8.74×10^{4} ±2.9×10^{3}	*564*	9.59×10^{4} ±3.5×10^{3}	*570*	8.26×10^{4} ±2.0×10^{3}	*572*	4.73×10^{4} ±8.1×10^{2}	*572*	6.61×10^{4} ±2.3×10^{3}	*571*	7.26×10^{4} ±1.7×10^{3}
4	*582*	7.77×10^{4} ±2.7×10^{3}	*546*	4.01×10^{5} ±5.6×10^{3}	*572*	1.15×10^{5} ±3.0×10^{3}	*548*	3.26×10^{5} ±1.4×10^{4}	*571*	1.01×10^{5} ±6.9×10^{3}	*551*	2.97×10^{5} ±1.9×10^{4}	*572*	1.03×10^{5} ±3.9×10^{3}	*581*	7.71×10^{4} ±1.5×10^{3}	*582*	8.40×10^{4} ±2.8×10^{3}	*581*	7.60×10^{4} ±2.1×10^{3}
5	*578*	4.51×10^{4} ±2.9×10^{3}	*521*	4.83×10^{5} ±3.0×10^{4}	*568*	7.85×10^{4} ±2.3×10^{3}	*530*	3.32×10^{5} ±3.2×10^{4}	*569*	6.75×10^{4} ±1.7×10^{3}	*535*	2.44×10^{5} ±1.3×10^{4}	*568*	6.51×10^{4} ±4.5×10^{3}	*569*	6.47×10^{4} ±1.5×10^{3}	*575*	5.33×10^{4} ±2.1×10^{3}	*576*	5.16×10^{4} ±1.5×10^{3}
6	*581*	4.40×10^{4} ±2.7×10^{3}	*531*	1.55×10^{6} ±6.9×10^{4}	*555*	1.31×10^{5} ±4.8×10^{3}	*531*	1.27×10^{6} ±4.4×10^{4}	*553*	1.29×10^{5} ±5.2×10^{3}	*532*	9.93×10^{5} ±3.0×10^{4}	*553*	1.40×10^{5} ±5.5×10^{3}	*545*	5.65×10^{5} ±2.3×10^{3}	*577*	5.73×10^{4} ±5.9×10^{3}	*581*	5.78×10^{4} ±4.9×10^{3}
7	*584*	5.09×10^{4} ±1.6×10^{3}	*536*	8.98×10^{5} ±3.1×10^{4}	*562*	1.13×10^{5} ±3.3×10^{3}	*537*	7.56×10^{5} ±2.7×10^{4}	*564*	1.05×10^{5} ±3.0×10^{3}	*539*	5.22×10^{5} ±1.7×10^{4}	*564*	8.64×10^{4} ±9.3×10^{3}	*567*	8.34×10^{4} ±1.1×10^{3}	*581*	5.43×10^{4} ±2.4×10^{3}	*583*	4.98×10^{4} ±2.0×10^{3}
8	*581*	4.51×10^{4} ±1.3×10^{3}	*541*	5.15×10^{5} ±1.5×10^{4}	*564*	7.81×10^{4} ±3.4×10^{3}	*545*	4.23×10^{5} ±9.3×10^{4}	*571*	6.48×10^{4} ±9.8×10^{2}	*546*	2.56×10^{5} ±1.8×10^{4}	*564*	7.73×10^{4} ±2.5×10^{3}	*577*	2.84×10^{4} ±1.3×10^{3}	*579*	3.84×10^{4} ±2.2×10^{3}	*580*	4.50×10^{4} ±8.4×10^{2}
9	*583*	3.81×10^{4} ±1.6×10^{3}	*536*	5.48×10^{5} ±8.8×10^{3}	*570*	6.20×10^{4} ±1.9×10^{3}	*542*	3.17×10^{5} ±8.0×10^{3}	*570*	5.89×10^{4} ±1.6×10^{3}	*540*	2.43×10^{5} ±1.1×10^{4}	*570*	5.87×10^{4} ±4.2×10^{3}	*580*	3.97×10^{4} ±7.7×10^{2}	*579*	3.77×10^{4} ±2.4×10^{3}	*581*	3.25×10^{4} ±1.1×10^{3}
10	*581*	4.41×10^{4} ±1.0×10^{3}	*536*	5.54×10^{5} ±1.9×10^{4}	*568*	7.97×10^{4} ±3.0×10^{3}	*540*	3.38×10^{5} ±3.1×10^{4}	*570*	7.25×10^{4} ±2.9×10^{3}	*543*	2.55×10^{5} ±1.9×10^{4}	*569*	7.15×10^{4} ±5.0×10^{3}	*579*	4.64×10^{4} ±7.4×10^{2}	*579*	4.35×10^{4} ±1.1×10^{3}	*579*	5.03×10^{4} ±1.9×10^{3}
11	*583*	3.15×10^{4} ±2.0×10^{3}	*538*	2.82×10^{5} ±2.3×10^{4}	*567*	6.03×10^{4} ±3.7×10^{3}	*542*	1.79×10^{5} ±6.6×10^{4}	*569*	6.08×10^{4} ±1.9×10^{3}	*548*	1.51×10^{5} ±4.6×10^{3}	*568*	5.64×10^{4} ±2.4×10^{3}	*577*	3.55×10^{4} ±8.3×10^{2}	*582*	3.89×10^{4} ±1.6×10^{3}	*580*	3.96×10^{4} ±1.4×10^{3}
12	*579*	6.71×10^{4} ±3.1×10^{3}	*531*	2.00×10^{6} ±9.7×10^{4}	*546*	4.49×10^{5} ±5.4×10^{3}	*531*	1.77×10^{6} ±6.3×10^{4}	*545*	4.46×10^{5} ±8.8×10^{3}	*532*	1.54×10^{6} ±2.5×10^{5}	*543*	4.80×10^{5} ±5.7×10^{3}	*538*	6.93×10^{5} ±2.1×10^{3}	*573*	1.02×10^{5} ±2.9×10^{3}	*575*	9.93×10^{4} ±1.9×10^{3}
13	*577*	5.78×10^{4} ±3.8×10^{3}	*536*	1.28×10^{6} ±5.7×10^{4}	*540*	3.43×10^{5} ±5.7×10^{3}	*536*	1.12×10^{6} ±1.8×10^{4}	*541*	3.29×10^{5} ±1.3×10^{4}	*536*	6.77×10^{5} ±1.7×10^{4}	*540*	3.94×10^{5} ±4.5×10^{3}	*545*	2.36×10^{5} ±2.0×10^{3}	*566*	8.27×10^{4} ±2.9×10^{3}	*572*	7.12×10^{4} ±1.5×10^{3}
14	*582*	5.08×10^{4} ±1.6×10^{3}	*536*	1.33×10^{6} ±1.1×10^{4}	*551*	1.74×10^{5} ±2.9×10^{3}	*536*	1.00×10^{6} ±3.0×10^{4}	*552*	1.72×10^{5} ±1.1×10^{4}	*536*	7.09×10^{5} ±5.5×10^{4}	*552*	1.64×10^{5} ±1.1×10^{4}	*541*	5.73×10^{5} ±3.0×10^{3}	*580*	4.78×10^{4} ±2.1×10^{3}	*581*	5.23×10^{4} ±1.6×10^{3}
15	*581*	5.32×10^{4} ±2.1×10^{3}	*543*	2.28×10^{5} ±7.3×10^{3}	*564*	9.45×10^{4} ±1.2×10^{3}	*558*	9.83×10^{4} ±3.0×10^{3}	*573*	6.61×10^{4} ±1.6×10^{3}	*574*	6.10×10^{4} ±3.1×10^{3}	*542*	8.98×10^{4} ±1.1×10^{4}	*512*	2.60×10^{6} ±6.5×10^{3}	*576*	5.20×10^{4} ±1.1×10^{3}	*570*	6.48×10^{4} ±1.5×10^{3}
16	*574*	5.76×10^{4} ±2.2×10^{3}	*567*	8.13×10^{5} ±1.7×10^{3}	*565*	9.52×10^{4} ±2.4×10^{3}	*569*	7.92×10^{4} ±8.0×10^{3}	*570*	6.60×10^{4} ±1.2×10^{4}	*571*	5.89×10^{4} ±3.3×10^{3}	*568*	7.74×10^{4} ±2.3×10^{3}	*573*	7.54×10^{4} ±1.0×10^{3}	*561*	7.69×10^{4} ±2.5×10^{3}	*572*	6.38×10^{4} ±1.8×10^{3}
17	*581*	5.09×10^{4} ±2.1×10^{3}	*557*	1.14×10^{5} ±5.5×10^{3}	*571*	8.24×10^{4} ±1.8×10^{3}	*569*	8.21×10^{4} ±2.1×10^{3}	*573*	7.86×10^{4} ±4.6×10^{3}	*574*	6.80×10^{4} ±6.0×10^{3}	*573*	8.41×10^{4} ±4.2×10^{3}	*576*	4.45×10^{4} ±4.2×10^{2}	*572*	7.54×10^{4} ±2.4×10^{3}	*549*	2.99×10^{5} ±2.5×10^{4}

Supporting Figure S5. Summary tables of (A) relative fluorescence increases and maximum wavelength shifts with all expressed PDZ domains and (B) fluorescence intensities at corresponding maximum wavelengths. (**A**) The most sensitive probes for each construct are highlighted in red. [a] RFI: Relative fluorescence increase. [b] Δλ: maximum wavelength shifts (nm), $\lambda\Delta=(\lambda_{max\ bound})-(\lambda_{max\ free})$. (**B**) Fluorescence intensities (arbitrary units) are reported for each peptide at the wavelength of maximum emission (λ_{max}, nm) either in the absence of domain (*apo*, $\lambda_{max\ free}$) or with each domain construct ($\lambda_{max\ bound}$). Final values are obtained by averaging the intensities of three independent measurements over a window of 5 nm centered around λ_{max}. [c] FI: Fluorescence intensity ± standard deviation.

Supporting Figure S6

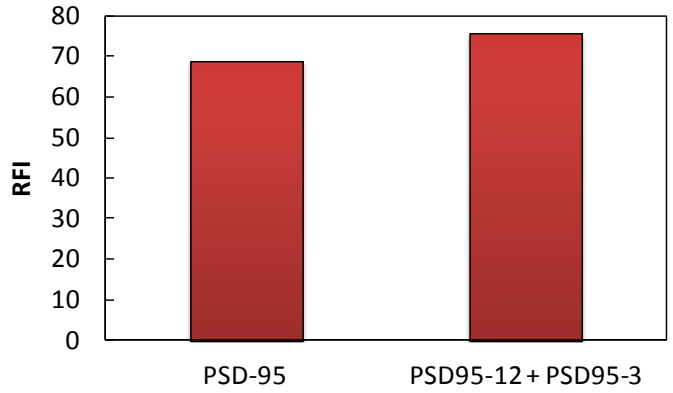

Supporting Figure S6. Comparison of full-length PSD-95 and a mixture of the expressed isolated PDZ domains. Relative fluorescence increase obtained with peptide **6** in PBS (2 μM) in absence and presence of either PSD-95 (10 μM in PBS) or PSD95-12 and PSD95-3 (each at 10 μM in PBS).

Supporting Figure S7

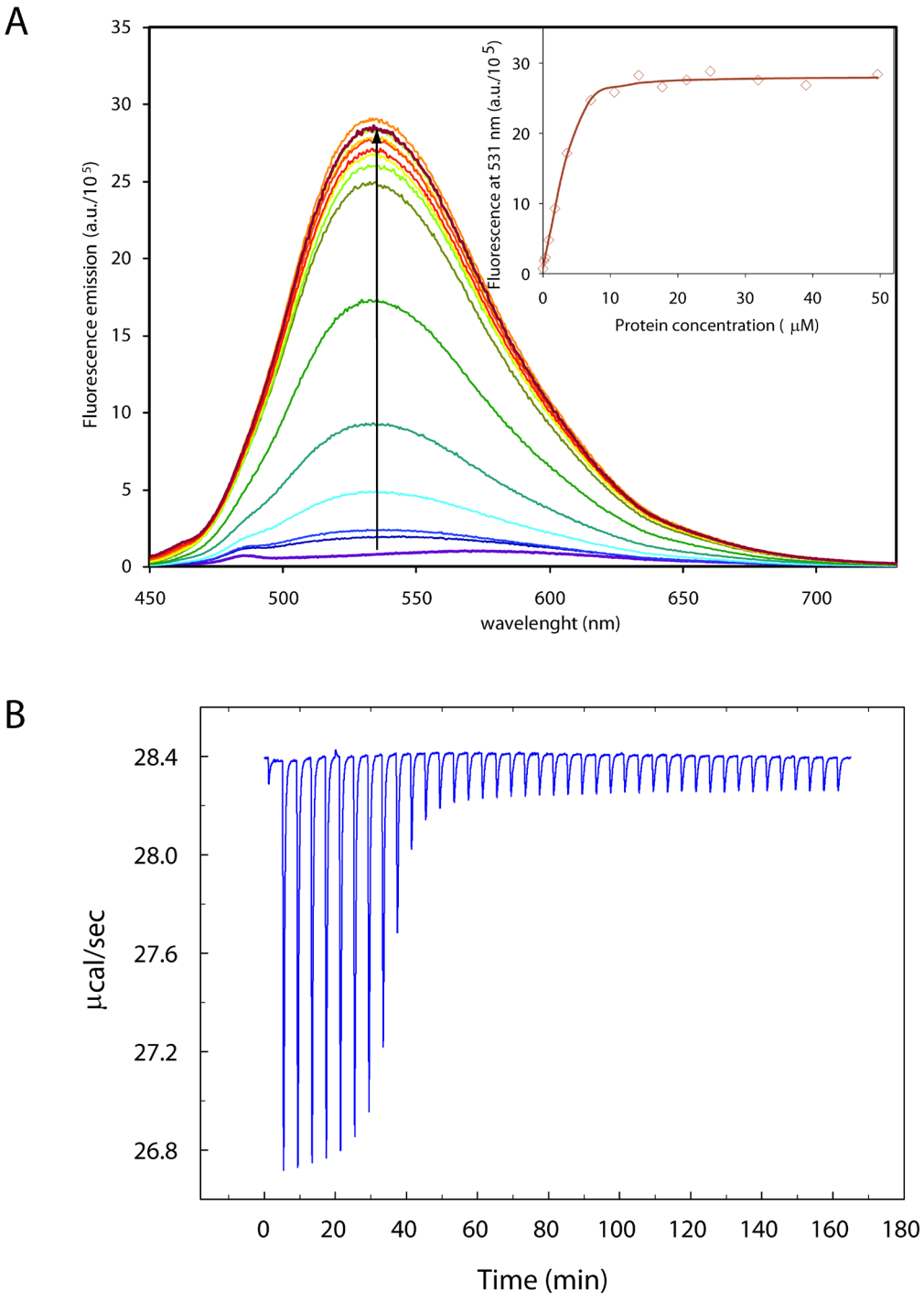

Supporting Figure S7. Representative example of titrations. (**A**) Fluorescence titration of peptide **12** (2 µM) vs PSD95-3 (varied from 0 to 49 µM) with insert of fitted data. (**B**) ITC thermogram of peptide **12** vs PSD95-3.

Supporting Figure S8

Entry	Sequence Origin	Sequence[a]	K_D (μM) (by ITC)	K_D (μM) (from lit.)	method[b]	Ref.
12	**Stargazin**	Ac-*NRR*NTANβRTTPV-COOH	0.59 ± 0.60	-		
18	**Stargazin**	Ac-φNTANRRTTPV-COOH	7.49 ± 1.07	7-15	FP	1
20	**CRIPT**	Ac-φDTKNYKQTSV-COOH	3.44 ± 0.50	3.39	FP	2

Supporting Table S8. Summary of ITC titrations and comparison with literature values for the third PDZ domain of PSD-95 (PSD95-3). [a] β = Dab(4-DMAP); φ = *p*-nitrophenylalanine. [b] FP = fluorescence polarization.

Supporting Figure S9

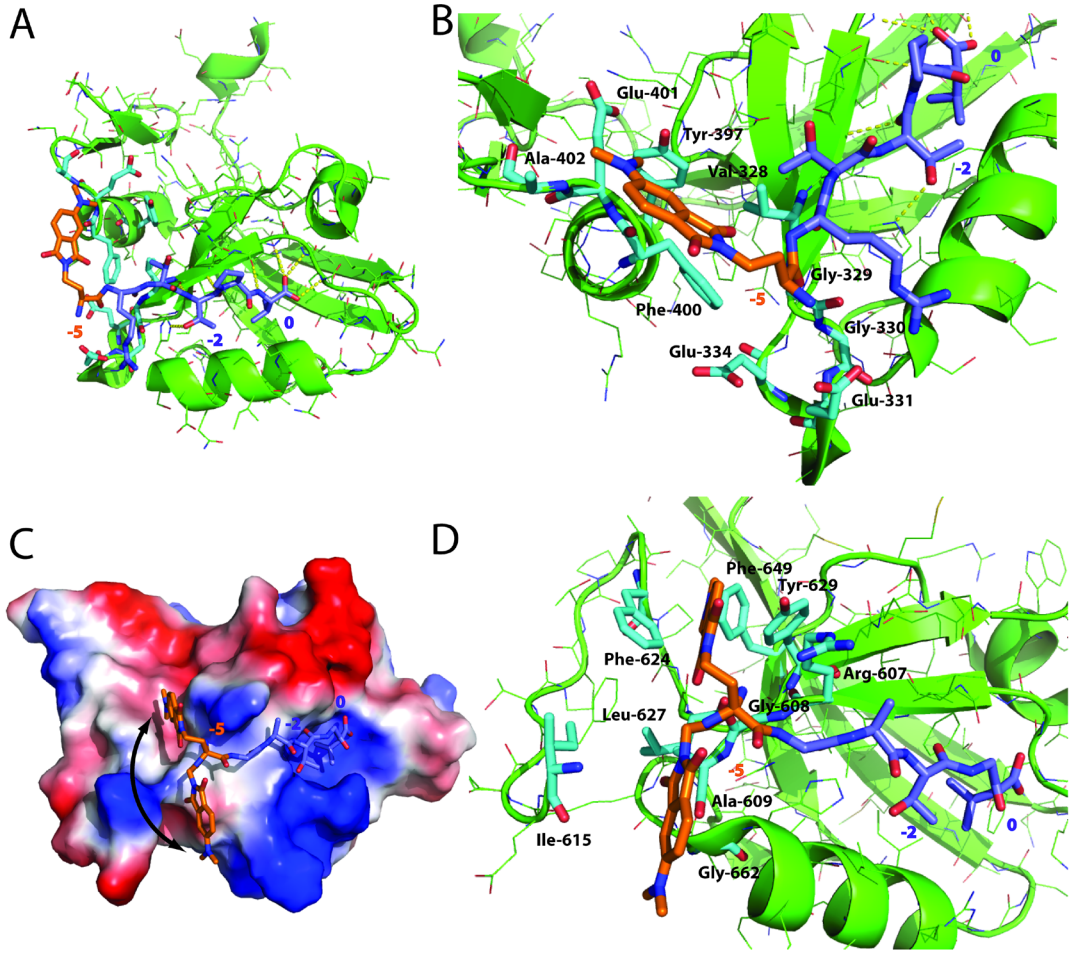

E

```
                                302                                                 339
PSD95-3                         LGEEDIPREP RRIVIHRGST GLGFNIVGG. .......... .EDGEGIFIS
SAP97-3                         LGDDEITREP RKVVLHRGST GLGFNIVGG. .......... .EDGEGIFIS
SAP102-3                        LAEEDFTREP RKIILHKGST GLGFNIVGG. .......... .EDGEGIFVS

Shank3 [from Shank1]            SHSDYVIDDK VAILQKRDHE GFGFVLRGAK AETPIEEFTP TPAFPALQYL
                                                      βB                        βC
                                340                                                 389
PSD95-3                         FILAGGPADL SGELRKGDQI LSVNGVDLRN ASHEQAAIAL KNAGQTVTII
SAP97-3                         FILAGGPADL SGELRKGDRI ISVNSVDLRA ASHEQAAAAL KNAGQAVTIV
SAP102-3                        FILAGGPADL SGELRRGDRI LSVNGVNLRN ATHEQAAAAL KRAGQSVTIV

Shank3 [from Shank1]            ESVDVEGVAW KAGLRTGDFL IEVNGVNVVK VGHKQVVGLI RQGGNRLVMK

                                390         402
PSD95-3                         AQYKPEEYSR FEA..
SAP97-3                         AQYRPEEYSR FEA..
SAP102-3                        AQYRPEEYSR FES..

Shank3 [from Shank1]            VVSVTRKPEE DSARR
```

Supporting Figure S9. Modeling of the PDZ domain-probe complexes and identification of the potential PDZ domain residues interacting with the 4-DMAP chromophore for PSD95-3 and Shank3. (**A**) and (**B**) model of probe **12** bound to PSD95-3 (based on PDB entry 1TP3). (**C**) and (**D**) model of probe **15** bound to Shank1 (based on PDB entry 1Q3P). (**E**) Sequence alignment of MAGUK third PDZ domains and Shank3 PDZ domain (PSD-95 numbering). Alignment of probes **12** and **15** with the complexed ligands indicates that, in both cases, the chromophore should be located at the end of the

binding groove in the proximity of the loop connecting β-sheets B and C (see reference 3 for a definition of the structure of PDZ domains). In the case of PSD95-3, a third α-helix from the N-terminal part of the domain is also potentially in close contact with 4-DMAP. The residues that could be interacting with the fluorophore (**E**) are conserved over members of the MAGUK family (SAP102-3 and SAP97-3, in green). However, the nature of these residues is highly variable and includes acidic, aliphatic and aromatic side chains. The region between the loop connecting β-sheets B and C and the third helix (-**Y**SR**FEA**-) seems to be the most likely position for the fluorophore. For Shank1/3, the loop connecting β-sheets B and C is longer than for PSD95-3 and, in the Shank1 structure, poorly resolved (yellow and gray lettering indicate residues that could not be assigned in 1Q3P). Modeling suggests that this loop is the main region of the domain that could interact with the chromophore. From the resolved amino acids, a few aromatic residues could be identified as potential interacting partners for the chromophore (in orange in the sequence alignment, identical in Shank1 and 3 sequences).

Overall, despite a similar positioning of 4-DMAP, the nature and local arrangement of the residues potentially involved in contacts with the probes fluorescent reporter are significantly different for MAGUK and Shank1/3. Furthermore, in both cases, no clearly defined hydrophobic clusters could be identified in the vicinity of the -5 position. As a consequence, while the modeling approach allowed us to locate the potential environment of 4-DMAP, it is not sufficient to identify the origin of the high fluorescence increase or even predict an optimal location for the fluorescent reporter group.

Supporting Methods

ABBREVIATIONS

HBTU 2-(1-*H*-Benzotriazol-1-yl)-1,1,3,3-tetramethyluronium hexafluorophosphate
HOBt 1-Hydroxy-benzotriazole
Dap L-2,3-Diaminopropionic acid
Dab L-2,4-Diaminobutyric acid
Orn L-Ornithine
MES 2-(N-Morpholino)ethanesulfonic acid
DHB 2,5-dihydroxybenzoic acid

PROBE SYNTHESIS

General

All reagents for peptide synthesis were of analytical grade. Amino acids and reagents were obtained from GenScript, NovabioChem and Sigma-Aldrich. Fmoc-Val/Leu/Ile-NovaSyn® TGT resins (0.20 mmol/g) were obtained from NovaBiochem and Fmoc-PAL-PEG-PS resin (0.20 mmol/g) was obtained from Applied Biosystems. 4-DMAP anhydride (4-dimethylaminophthalenedicarboxilic anhydride) was synthesized according to the previously reported methods.[4]

Peptide synthesis (SPPS) and fluorophore insertion

Peptides were obtained by either manual synthesis or with an automated synthesizer (Advanced ChemTech automated synthesizer model 396 Ω) by using standard Fmoc-based solid phase peptide synthesis procedures. Typically manual synthesis was performed on a 0.04 to 0.02 mmol scale with TGT resin (~0.2 mmol/g) or PAL-PEG-PS resin (~0.2 mmol/g), using standard Fmoc-protected amino acid (6 equivalents), HBTU/HOBt as coupling reagents (6 equivalents each) and DIPEA (12 equivalents) in DMF or NMP. Coupling steps were conducted with a 50 mM amino acid solution (~1 mL per 100 mg of resin) for 1 hour. Fmoc group deprotection was performed after each coupling step with a 20% solution of 4-methyl-piperidine in DMF (vol/vol) for 3 × 5 minutes. After removal of the N-terminal Fmoc group, the resulting free amine was capped with an acetyl group by using an acetic anhydride/pyridine solution (0.15 M each in DMF).

Peptides incorporating the 4-DMAP environment-sensitive fluorophore were synthesized using the on-resin derivatization approach previously reported.[5] Briefly, an Alloc-protected diaminoacid (Fmoc-L-Dap(Alloc)-OH, Fmoc-L-Dab(Alloc)-OH or Fmoc-L-Orn(Alloc)-OH from AnaSpec) was initially incorporated in the SPPS steps. After capping of the N-terminal amino group of the peptide sequence, the Alloc-protecting group was removed by resuspending the resin in dry dichloromethane (20 mM in peptide) with a stream of N_2 bubbling through the solution for 5 minutes. $Pd(PPh_3)_4$ (0.8 equiv.) and phenylsilane (25 equiv.) were then added to the solution which was maintained under N_2 bubbling for another 15 minutes. The resin was then washed with dichloromethane and DMF. The degassing/deprotection cycle was repeated two additional times. The resin containing the free amine was reacted with a solution of the anhydride form of 4-DMAP (4-*N*,*N*-dimethylaminophthalic anhydride, 2 equiv., 50 mM) and DIPEA (4 equiv.) in NMP. The mixture was allowed to stir overnight. The resin was then washed with DMF and dichloromethane and ring closure was performed by using a solution of HBTU/HOBt (6 equiv., 50 mM) in NMP or DMF with DIPEA (12 equiv.) for 2 hours. The resin was then washed with DMF and dichloromethane. The washing/coupling cycle was repeated two additional times in order to achieve full ring closure.

Peptides were deprotected and cleaved from the resin with a TFA/H_2O/TIPS (95:2.5:2.5) cleavage cocktail for 2 h 30 min to 3h. TFA was evaporated until the peptides precipitated. The peptides were then triturated and precipitated in cold ether before purification by reverse phase HPLC on a semi-preparative

column (YMC-Pack Pro C_{18}, ODS-A 5/120, 250×20 mm) in water (0.1% TFA) using an acetonitrile (0.1% TFA) gradient and monitoring at 228 nm and 350 nm. Peptides were stored in lyophilized form at -80 ^{0}C until use.

Peptide characterization (HPLC, MALDI) and quantification
Peptide identity was confirmed by MALDI-TOF mass spectroscopy (MALDI-TOF, PerSeptive Biosystems Voyager) using DHB as a matrix. Purity was assessed by analytical reverse phase HPLC (YMC C_{18}, ODS-A 5/120, 250×4.6 mm) using a standard gradient (5% acetonitrile containing 0.1% TFA for 5 min followed by 5-95% acetonitrile containing 0.1% TFA over 35 min in water containing 0.1% TFA at a flow rate of 1 mL.min^{-1}). All the peptides were more than 95% pure as judged by analytical HPLC. The final peptides were quantified using molar extinction coefficients of either 4-DMAP ($\varepsilon_{421\ nm}$ = 6480 M^{-1}.cm^{-1} in water) or p-nitrophenylalanine ($\varepsilon_{280\ nm}$ = 12500 M^{-1}.cm^{-1}).

BUFFERS

Phosphate buffer saline solution (PBS 10x)
10x PBS consists of 1.5 M NaCl, 50 mM Na_2HPO_4 and 50 mM NaH_2PO_4 in distilled water, adjusted to pH 7.4. A 1x solution is obtained by a ten-fold dilution of the 10x in distilled water. Solvents were filtered before spectroscopic applications (with 0.45 μm PVDF membranes).

MES buffer (10x)
10x MES buffer consists of 1 M NaCl and 100mM MES in distilled water, adjusted to pH 6.9. A 1x solution is obtained by a ten-fold dilution of the 10x in distilled water.

PDZ DOMAIN CLONING AND EXPRESSION

Cloning – PDZ domains and rationale on tandem domain cloning
The cDNA encoding for the genes used for PDZ domains subcloning were provided by Daniel Choquet (Laboratoire Physiologie Cellulaire de la Synapse; PSD-95, SAP-102, GRIP-1, PICK-1 and Shank-3) and Morgan Sheng (Picower Institute; SAP-97). The PDZ domains of interest were cloned into the pGEX-4T-2 vector (GE Healthcare) using BamHI and XhoI restriction sites. Primers were designed to subclone the PDZ domain(s) as defined by the ExPASy Proteomics Server (UniProtKB/Swiss-Prot database) plus 5 to 10 extra flanking amino acids. Primers incorporated a TEV cleavage site between GST and the domains as well as a FLAG tag at the C-terminus.
Multiple studies have shown that closely grouped PDZ domains, or "tandem PDZ domains", interact together with resulting effects on both the structural and functional properties. For instance, both GRIP1 1st and 5th PDZ domains require the presence of neighboring domains (2nd and 4th respectively) to fold properly and bind to their targets (Fras1 for the 1st domain and GluR2 for the 5th).[6-8] To a lesser extent, interactions between domains 1 and 2 of PSD-95[9] and SAP-97[10] have been observed, albeit no evidence for differences in binding to cognate peptides were shown for isolated or tandem domains. Tandem PDZ domains should be considered as supramodular entities where both domains are required for proper function. Recombinant isolated PDZ domains when cloned out of a tandem structure might therefore adopt a different conformation, which could affect their binding properties and the local microenvironment sensed by environment-sensitive probes. As a precautionary measure and for consistency, the tandem PDZ domains of PSD-95, SAP-97, SAP-102 and GRIP-1 (first two domains of MAGUKs and domains 4 and 5 of GRIP-1) were therefore cloned together in order to preserve their native structure and avoid artifacts due to improper folding of artificially isolated domains.
The first two PDZ domains of PSD-95, PSD95-12 (residues 61 to 249, from UniProtKB/Swiss-Prot entry P31016), were PCR-amplified using the primers 5'-CGG GAT CCG AGA ATT TGT ATT TTC AGG

GCA TGG AGT ATG AGG AGA TCA CAT TGG and 5'-CCG CTC GAG TTA CTT ATC GTC ATC GTC TTT GTA GTC GGC ATT GCT GGG CTT GGC CAC CTT T.
The third PDZ domain of PSD-95, PSD95-3 (residues 302 to 402, from UniProtKB/Swiss-Prot entry P31016), was PCR-amplified using the primers 5'-CGG GAT CCG AGA ATT TGT ATT TTC AGG GCC TGG GGG AGG AAG ACA TTC CCC GGG and 5'-CCG CTC GAG TTA CTT ATC GTC ATC GTC TTT GTA GTC GGC CTC GAA TCG ACT ATA CTC TTC T.
The first two PDZ domains of SAP-102, SAP102-12 (residues 139 to 338, from UniProtKB/Swiss-Prot entry Q62936), were PCR-amplified using the primers 5'-CGG GAT CCG AGA ACC TGT ACT TCC AGG GCA ATG GCA GTG ATG GCA TGT TCA AGT and 5'-CCG GAA TTC TTA CTT GTC GTC ATC GTC CTT GTA GTC CAT GTC GTT GAG GTG GAG ACT GCC.
The third PDZ domain of SAP-102, SAP102-3 (residues 393 to 493, from UniProtKB/Swiss-Prot entry Q62936), was PCR-amplified using the primers 5'-CGG GAT CCG AGA ACC TGT ACT TCC AGG GC CTG GCT GAG GAA GAC TTT ACC A and 5'-CCG GAA TTC TTA CTT GTC GTC ATC GTC CTT GTA GTC GGA TTC AAA GCG ACT GTA CTC.
The first two PDZ domains of SAP-97, SAP97-12 (residues 213 to 413, from UniProtKB/Swiss-Prot entry Q811D0), were PCR-amplified using the primers 5'-CGG GAT CCG AGA ACC TGT ACT TCC AGG GCG ATG CAG ATT ATG AAT ATG AGG and 5'-CCG GAA TTC TTA CTT GTC GTC ATC GTC CTT GTA GTC GCC ATC ATT TAT ATA CAT ACT.
The third PDZ domain of SAP-97, SAP97-3 (residues 455 to 555, from UniProtKB/Swiss-Prot entry Q811D0), was PCR-amplified using the primers 5'-CGG GAT CCG AGA ACC TGT ACT TCC AGG GCC TTG GAG ATG ATG AGA TCA CTA and 5'-CCG GAA TTC TTA CTT GTC GTC ATC GTC CTT GTA GTC AGC TTC AAA ACG ACT GTA CTC T.
The 4th and 5th PDZ domains of GRIP-1, GRIP1-45 (residues 430 to 663, from UniProtKB/Swiss-Prot entry P97879), were PCR-amplified using the primers 5'-CGG GAT CCG AGA ATT TGT ATT TTC AGG GCT CTA CTA GTC CAC GAG GAA CCA TGA and 5'-CCG CTC GAG TTA CTT ATC GTC ATC GTC TTT GTA GTC CTC TTG CTC ATC TGA GTT ATC TTC A.
The PDZ domain of PICK-1 (residues 11 to 113, from UniProtKB/Swiss-Prot entry Q9EP80), was PCR-amplified using the primers 5'-CGG GAT CCG AGA ATT TGT ATT TTC AGG GCG AGG ATA AAT TAG GAA TCC CC and 5'-CCG CTC GAG TTA CTT ATC GTC ATC GTC TTT GTA GTC GGA CAT GCC CTG CTT AGG GTC.
The PDZ domain of Shank-3, Shank3 (residues 633 to 747, from UniProtKB/Swiss-Prot entry Q9JLU4), was PCR-amplified using the primers 5'-CGG GAT CCG AGA ACC TGT ACT TCC AGG GCT CAC ACA GTG ATT ATG TCA TTG ATG and 5'-CCG GAA TTC TTA CTT ATC GTC ATC GTC CTT GTA GTC TGC GCC GAG CAC TAT CCT CCT CTG.
The PCR-amplified inserts were digested with either BamHI/XhoI or BamHI/EcoRI and ligated into a BamHI/XhoI- or BamHI/EcoRI-digested pGEX-4T-2 vector.

Cloning – PSD-95
PSD-95 (UniProtKB/Swiss-Prot entry P31016) was PCR-amplified using the primers 5'-CGG AAT TCA TGG ACT GTC TCT GTA TAG T and 5'-CCG CTC GAG GAG TCT CTC TCG GGC TGG GAC. The PCR-amplified insert was digested with EcoRI/XhoI and ligated into an EcoRI/XhoI-digested pET24a vector (Novagen, C-terminal His_6-tag).

Expression and purification of the recombinant PDZ domains (GST fusion proteins)
E. Coli BL21 codon plus ™ (DE3)-RIL or RP cells were transformed with each of the GST fusion protein expression plasmids. Cells were amplified in 0.5 L of an auto-inducing medium[11] (ZYM-5052, see reference 11 for detailed composition) first at 37 ºC for 4 hours followed by 12 hours at 16 ºC. Cells were harvested by centrifugation and the pellet was resuspended in lysis buffer (100 mM EDTA, 10% glycerol, 1% TritonX-100, 1 mg/mL lysozyme in PBS, pH 7.4) containing protease inhibitor cocktail III (Calbiochem). Cells were lysed by ultrasonication (Branson Sonifier 450 at 50% power with a 40% duty cycle for 4 min at 4 ºC). After addition of 1 mL of a 1 mM solution of DTT in water, the lysate was

cleared by centrifugation (15,334 g, 40 minutes, 4 ºC). The GST-fusion proteins were purified with about 5 mL of Glutathione Sepharose™ 4 Fast Flow (GE Healthcare) by batch-binding. The bound proteins were washed with 20 volumes of PBS (pH 7.4) and eluted with 2 volumes of a 10 mM glutathione in 50 mM Tris (pH 8) solution. Fractions were analyzed by 12% SDS-PAGE followed by Coomassie staining and Western blotting (anti-FLAG). Fractions containing the protein were pooled and dialyzed against PBS (pH 7.4). Protein concentrations were measured using either the BCA assay (Pierce) with BSA as the reference standard or by determining the absorption at 280 nm in 6 M guanidinium chloride. Purified PDZ domains were aliquoted, flash-frozen and stored at −80 °C in PBS (pH 7.4) until use.

Expression and purification of recombinant PSD-95

E. Coli BL21 codon plus ™ (DE3)-RIL cells were transformed with the PSD-95 expression plasmid. Cells were amplified in 0.5 L of an auto-inducing medium (ZYM-5052, see reference 10 for detailed composition) first at 37 ºC for 4 hours, followed by 12 hours at 15 ºC. Cells were harvested by centrifugation and the pellet was resuspended in lysis buffer (10% glycerol, 1% TritonX-100, 1 mg/mL lysozyme in 50 mM TrisOAc, 300 mM NaCl and 5 mM imidazole, pH 8) containing protease inhibitor cocktail III (Calbiochem). Cells were lysed by ultrasonication (Branson Sonifier 450 at 50% power with a 40% duty cycle for 4 min at 4 ºC). The lysate was cleared by centrifugation (15,334 g, 40 minutes, 4 ºC). The protein was purified with about 5 mL of Ni-NTA agarose (Qiagen) by batch-binding. The bound protein was washed with 10 volumes of 50 mM TrisOAc, 300 mM NaCl (pH 8) with an increasing amount of imidazole (from 0 to 25 mM) and eluted with 2 volumes of a 50 mM TrisOAc, 300 mM NaCl and 250 mM imidazole solution (pH 8). Fractions were analyzed by 12% SDS-PAGE followed by Coomassie staining and Western blotting (anti-His_6). Fractions containing the protein were pooled and dialyzed against PBS (pH 7.4). Protein concentration was measured using either the BCA assay (Pierce) with BSA as the reference standard or by determining the absorption at 280 nm in 8 mM guanidinium chloride. The purified protein was flash-frozen and stored at −80 °C in PBS (pH 7.4) until use.

FLUORESCENCE STUDIES

Materials and general methods

Fluorescence spectra were recorded on a Fluoromax 3 instrument (Horiba Jobin Yvon) in 1 cm path length quartz cells (100 µL nominal volume from Starna Cells). All measurements were performed at a constant temperature of 25 °C. The spectra were corrected for emission intensity by using manufacturer-supplied correction factors. Slit widths were 3 nm for excitation and 6 nm for emission. The 4-DMAP fluorophore was excited at 421 nm and the spectra were recorded between 432 nm and 730 nm (0.5 nm increments and 0.1 s integration time).

Relative fluorescence increases

The fluorescence increase measurements were performed at 25 °C in PBS buffer (pH 7.4) comparing solutions of (1) 2 µM of 4-DMAP-containing peptide alone in PBS and (2) 2 µM of 4-DMAP-containing peptide with 20 µM of PDZ domain construct in PBS. Blanks consisting of PBS for (1) and PBS with 20 µM of the corresponding PDZ domain construct for (2) were subtracted from the respective spectra. Each final spectrum resulted from the average of at least three independent runs. The relative fluorescence increases for each series of peptides and PDZ domain(s) were evaluated by comparing the resulting averaged fluorescence emission intensities of (2) and (1) at the wavelength of maximal emission of (2). Ratios were calculated over a 5 nm range centered on the wavelength of maximal emission of (2) and the values were averaged to yield the reported final ratio. In the case of full-length PSD-95, the protein was used at 10 µM and compared to a mixture of PSD95-12 and PSD95-3 each at 10 µM.

Fluorescence titration

For each titration, the peptide concentration was kept constant (around 1 to 20 µM) and the protein concentration was varied from values lower or close to the anticipated K_D to saturation of the

fluorescence signal increase. A 150 or 130 µL solution in PBS (pH 7.4) [or MES (pH 6.9)] was prepared for each protein concentration. Dissociation constants were evaluated using SPECFIT/32™ Global Analysis System for Windows (version 3.0.39) after averaging at least three independent titrations and taking into account wavelengths from 432 to 730 nm. Data obtained with PSD-95 tandem PDZ domains (PSD95-12) were fitted as with single domains to yield apparent dissociation constants.

Competitive titrations.
Competition experiments were conducted on 450 µL of a PBS (pH 7.4) solution containing 5 µM of fluorescent peptide and 5 µM of PDZ domain. The non-fluorescent peptide solution was added sequentially in small volumes to achieve a range of concentrations from 1 nM to 2 mM. The titrations were done at least in triplicate and averaged. The K_i were obtained by fitting the relative fluorescence increase (RFI, obtained as described above) of the averaged spectrum to the logarithm of the non-fluorescent peptide concentration (Log[nFP], Molar) using the Competitive Binding: One Site model from GraphPad Prism 5 software with the following equations:

$$Log(EC50) = Log\left(10^{Log\,K_i} * \left(1 + \frac{[FP]}{K_D^{Fluo}}\right)\right)$$

$$RFI = min_{RFI} + \frac{(max_{RFI} - min_{RFI})}{(1 + 10^{(Log\,[nFP] - LogEC\,50)})}$$

where [FP] is the concentration of the fluorescent peptide (constant), K_D^{Fluo} is the dissociation constant of the fluorescent peptide with the corresponding PDZ domain (constant, same unit as [FP]), min_{RFI} and max_{RFI} correspond respectively to 1 (i.e., no fluorescence increase) and the RFI in the absence of competitive ligand.

ISOTHERMAL TITRATION CALORIMETRY STUDIES

Titrations were conducted on a VP-ITC MicroCalorimeter (MicroCal). The PDZ domains were dialyzed against MES buffer (pH 6.9). The protein and peptide samples (prepared in the same buffer) were degassed separately for 10 min under vacuum with stirring. The PDZ domain (20 to 50 µM, 1.8 mL) was loaded into the sample cell and a 400 to 1000 µM peptide solution (250 µL) was drawn into the syringe. Typically 30 to 50 injections were programmed, with the first injection volume set at 0.5 µL (1 s injection) and the remaining at 7 µL (in 45 injections of 14 s each). The spacing between injections was 240 s. The reference power was 30 µcal/s with an initial delay of 1 min. Experiments were conducted at 25 °C with a stirring speed of 500 rpm. The raw data were collected and analyzed by ORIGIN software (MicroCal). The binding constants were determined by non-linear least squares fitting using a One Set of Binding Sites model.

STRUCTURAL MODELING

Modeling was conducted with X-ray crystallographic structures of the PDZ domains of interest bound to ligands using PyMOL v1.1 (DeLano Scientific LLC). We focused our study on the probes that produced the most impressive fluorescence increases, **12** and **15**, for PSD95-3 and Shank3 respectively. Of note, Shank1 PDZ domain, and not Shank3, is the only structure currently available in the Protein Data Bank, but considering the high sequence identity and homology between the two proteins (77% and 87% respectively), we used it as a starting point for the model of Shank3. Similarly, we considered that modeling on PSD95-3 would also apply to SAP97-3 and SAP102-3. The last six amino acids of peptides **12** and **15** were docked into X-ray crystallographic structures of ligand-bound PSD95-3 (1TP3) and

Shank1 (1Q3P) respectively by aligning the probe peptide backbone to the crystallized ligand (KKETPV for 1TP3 and EAGTRL for 1Q3P) and replacing similar/identical side chain residues. In the case of the fluorescent amino acid, only the backbone amide was aligned to the resolved ligand and the linker bonds were freely rotated to estimate the domain residues within reach of the 4-DMAP chromophore.

REFERENCES

(1) Dakoji, S.; Tomita, S.; Karimzadegan, S.; Nicoll, R. A.; Bredt, D. S. *Neuropharmacology* **2003**, *45*, 849-856.
(2) Lim, I. A.; Hall, D. D.; Hell, J. W. *J. Biol. Chem.* **2002**, *277*, 21697-21711.
(3) Doyle, D. A.; Lee, A.; Lewis, J.; Kim, E.; Sheng, M.; MacKinnon, R. *Cell* **1996**, *85*, 1067-1076.
(4) Sainlos, M.; Imperiali, B. *Nat. Protoc.* **2007**, *2*, 3219-3225.
(5) Sainlos, M.; Imperiali, B. *Nat. Protoc.* **2007**, *2*, 3201-3209.
(6) Long, J.; Wei, Z.; Feng, W.; Yu, C.; Zhao, Y. X.; Zhang, M. *J. Mol. Biol.* **2008**, *375*, 1457-68.
(7) Zhang, Q.; Fan, J.-S.; Zhang, M. *J. Biol. Chem.* **2001**, *276*, 43216-43220.
(8) Feng, W.; Shi, Y.; Li, M.; Zhang, M. *Nat. Struct. Biol.* **2003**, *10*, 972-978.
(9) Long, J. F.; Tochio, H.; Wang, P.; Fan, J. S.; Sala, C.; Niethammer, M.; Sheng, M.; Zhang, M. J. *J. Mol. Biol.* **2003**, *327*, 203-214.
(10) Goult, B. T.; Rapley, J. D.; Dart, C.; Kitmitto, A.; Grossmann, J. G.; Leyland, M. L.; Lian, L. Y. *Biochemistry* **2007**, *46*, 14117-28.
(11) Studier, F. W. *Protein Expres. Purif.* **2005**, *41*, 207-234.